Polymeric micropump with SU-8 check valves assembled by lamination technique

T-Q. Truong and N-T. Nguyen

MPE School, Nanyang Technological University, Singapore, quangtt@pmail.ntu.edu.sg

ABSTRACT

This paper presents the first micropumps assembled using polymeric lamination technology. Each pump consists of two 100-μm-thick, 10-mm-diameter SU-8 discs; two 1.5-mm-thick, 15-mm-diameter polymethylmethacrylate (PMMA) discs; and one piezo disc. The SU-8 parts were fabricated by a two-mask polymeric surface micromachining process. The PMMA parts were machined from a PMMA sheet by CO_2-laser. The pump was assembled using adhesive bonding. The adhesive tapes were cut by the same laser system. With a drive voltage of $\pm$ 150 V the fabricated micropumps have been able to provide flow rates up to 2.9 ml/min and back pressures up to 1.6 m of water. The pump design and the polymeric technologies prove the feasibility of making more complex microfluidic systems based on the presented lamination approach.

Keywords: microfluidics, micropumps, SU-8, polymeric laminate technology

1 INTRODUCTION

In recent years, lab on a chips (LOC) has been attracting the interests of both industry and research community. Commercial LOCs are often made of polymers to achieve low cost, good biocompatibility, and good chemical resistance [1]. The transport of fluid in LOCs can be provided by micropumps. Therefore, there is a need for polymeric micropump designs which can easily be integrated in the polymeric fabrication process of LOCs. In [2], we reported such a micropump, which was fabricated with a layered concept. The pump consisted of SU-8 check valves fabricated by polymeric surface micromachining techniques, and polymethylmethacrylate (PMMA) plates machined by milling tools. Four bolts were used to fix the structure.

This paper presents an improved version of the above mentioned pump. First, three new valves with sealing ring have been designed in order to reduce leakage and to lower spring constants. Second, laser micromachining was used to fabricate PMMA plates and adhesive layers. Third, low-temperature adhesive bonding was used for laminating different polymer layers. The lamination technique is flexible and can be extended to more complex microfluidic systems.

2 MICROPUMP DESIGN

2.1 The pump structure

The pump consists of five structural layers: the piezo bimorph disc, the top PMMA plate, two SU-8 discs, and the bottom PMMA plate. These layers are bonded by four adhesive layers, Figure 1. The piezo bimorph disc is a brass plate 15 mm in diameter and 100 μm thick. A 90μm-thick layer of piezo ceramic is glued on top of the brass plate. The piezo bimorph disc works as both the actuator and the pump membrane. The top and bottom PMMA plates are identical. Each plate measures 15 mm in diameter and 1.5 mm thick. It has two through-holes for fluid access, and two other alignment holes. The fluid accesses are 0.6 mm in diameter. The alignment holes have a diameter of 1.6 mm. The space between the top PMMA plate and the piezo disc defines the pump chamber. Two fluid accesses of the bottom PMMA plate are fitted with two metal needles used as inlet and outlet. The two SU-8 discs are identical, 10 mm in diameter and 100 μm thick. The top SU-8 disc contains the outlet valve while the inlet valve is implemented in the bottom disc. Two alignment holes are incorporated in each of the PMMA plates and SU-8 discs.

2.2 Design of the SU-8 check valves

Each SU-8 disc consists of one check valve, one inlet hole and two alignment holes, Figure 2. The check valve consists of a 1-mm valve disc suspended on N folded beams, which have a cross section of 100 μm $\times$ 100 μm. The beams work as valve springs connected in parallel [1]. The valve disc has a sealing ring, which is 100 μm thick. Its outer diameter and inner diameter are 0.9 mm and 0.6 mm, respectively. The ring offsets the 50 μm gap, which was created by the adhesive layer, between the valve disc and the fluid access holes. The ring also creates a pre-loaded condition for the springs to reduce leakage. Figure 3 depicts the three valves implemented in the micropumps reported in this paper. The details on the designs and geometrical parameters are shown in Figure 3.

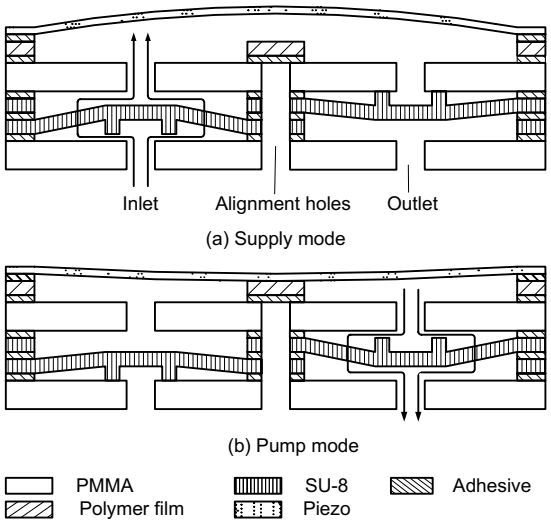

Figure 1: Schematic of the pump structure and is operation (not to scale). (a) Supply mode; (b) Pump mode.

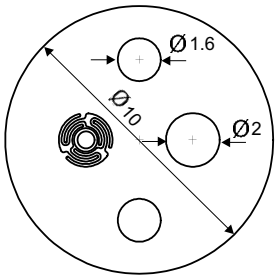

Figure 2: The geometry of the SU-8 disc (dimensions are in mm).

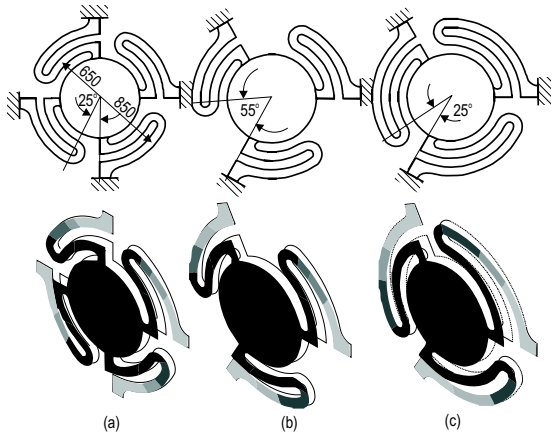

Figure 3: Three different valve designs result in three different spring constants (dimensions are in microns). Results obtained by FEM. (a) Valve 1, 4 springs, k = 927 N/m; (b) Valve 1, 3 springs, k = 691 N/m; (c) Valve 3, 3 extended springs, k = 286 N/m.

Numerical simulation with ANSYS was used to find the spring constants of the valves. A pressure of 3000 Pa was applied on the valve disc. The Young's modulus of SU-8 was assumed to be 4.02×10^9 Pa. The spring constant was determined by the force and the simulated displacement (1).

$$k = \frac{F}{\delta} = \frac{p\pi r^2}{\delta}, \tag{1}$$

where k is the spring constant, F is the force applied on the valve disc, p is the pressure, r is the radius of the valve disc, and δ is the displacement. The results in Figure 3 show that Valve 3 (c) is three and two times softer than Valve 1 and Valve 2, respectively.

3 FABRICATION

3.1 SU-8 disc

The SU-8 discs were fabricated using a two-mask polymeric surface micromachining process, described in details in [1]. The process started with spin-coating SU-8 2100 photoresist (Microchem Corp., USA) on silicon, Figure 4a. This first SU-8 was then soft baked and exposed to UV light using the first mask containing all features of the SU-8 disc except the ring, Figure 4b. The intended thickness of this SU-8 film was 100 μm. After hard baking, a second 100-μm-thick SU-8 layer was spin-coated on top of the first layer. After a soft-baking step, the second mask containing the ring design was used for the second exposure, Figure 4c. The second mask was aligned to the first SU-8 layer using alignment marks. Even though the first SU-8 layer had not been developed, the alignment marks were still visible. The visible alignment marks were made possible by the different optical indices between cross-linked SU-8 and the unexposed area. With this two-mask process, we achieved an accuracy of 10μm, which satisfied our application. After the second UV exposure, the two SU-8 layers were hard baked and cooled down to room temperature. They were then developed using propylene glycol methyl ether (PGMEA), Figure 4d. In the final steps, the SU-8 discs were released in 30% KOH solution. Etch access created by many circular holes on the discs allows fast under etching. The circular shapes and the smooth designs circumvents the anisotropic characteristics of the KOH etch process. After releasing the SU-8 discs were cleaned with DI (deionized water) water and dried with nitrogen.

Figure 5 shows the SEM (scanning electron microscopy) images of Valve 2 and Valve 3.

3.2 PMMA and adhesive parts

The PMMA plates were designed in Autocad and sent to a laser cutter (Universal Laser Systems, M-300,

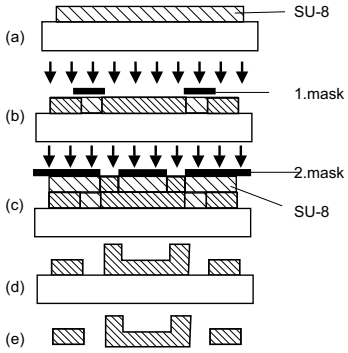

Figure 4: Process steps for the SU-8 valve disc

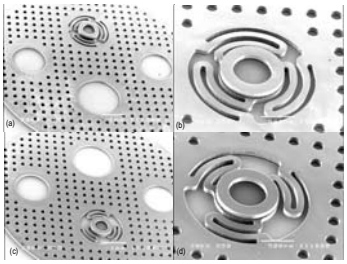

Figure 5: SEM picture of SU-8 check valves. (a) Top view, whole SU-8 disc, Valve 2; (b) Close-up of Valve 2; (c) Top view, whole SU-8 disc, Valve 3; (d) Close-up of Valve 3

25 W). The system can deliver a maximum laser power of 25 W and a maximum scanning velocity of 640 mm/s at a resolution of 1000 dpi. The power and the cutting speed for the PMMA parts were set at 9% and 1.1% of the maximum values, respectively. The material for the plates was a 1.5-mm-thick PMMA sheet (extrusion type).

The adhesive parts were cut out from a transfer adhesive tape (Adhesives Research, Inc, Arclad 8102 transfer adhesive). The transfer adhesive tape consists of a carrier and a 50-μm-thick adhesive layer. The laser power and the cutting speed for the adhesive tape were set at 1% and 1.1% of the maximum values respectively.

The polymer layer covering the alignment holes was cut out from a 100-μm-thick overhead projector transparency sheet (3M, PP2500) covered by the transfer adhesive tape. The laser power and cutting speed for these layers was set at 3% and 1.1% of the maximum values.

3.3 Assembly procedure

Figure 6 shows the assembly sequences of the micropump. First, the bottom PMMA plate was slotted into the alignment pins; followed by the first adhesive disc with the carrier facing up. The two layers were then pressed to bond. The carrier was then removed using two needles. Next, the bottom SU-8 disc with the sealing ring facing down was placed on the stack. Subsequently, the second adhesive disc was laminated on top

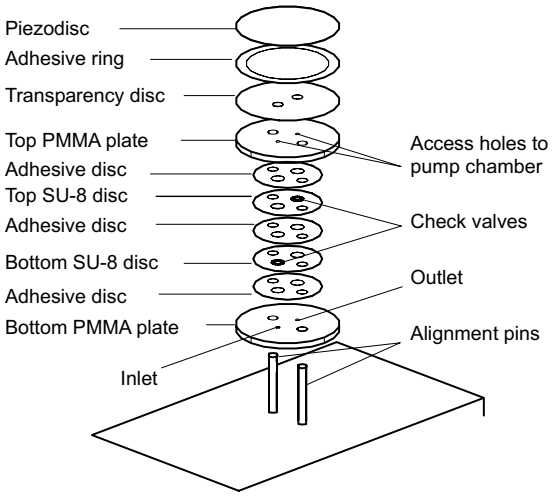

Figure 6: Lamination assembly concept of the micropump.

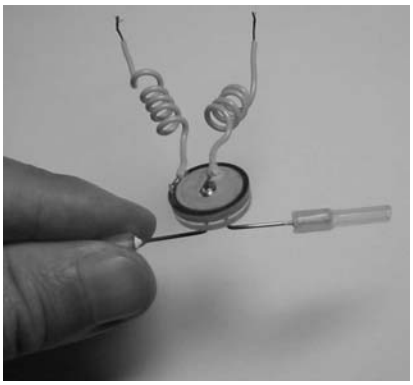

Figure 7: The assembled micropump.

the SU-8 disc; its carrier was then removed. In the next step, the top SU-8 disc with its ring facing up was assembled. The third adhesive later was laminated in the same manner as for the first two. The top PMMA plate was then placed on top of the stack. The whole stack was pressed to achieve good bonding. The bonded stack was then removed from the alignment pins. The carrier of the polymeric disc was removed. In the next step, the polymer layer covering the alignment holes was aligned to and pressed against the top PMMA plate. Next, the adhesive ring with the adhesive layer facing down was placed on top the polymer disc. The carrier of the ring was removed, ready to bond with the piezo disc. The piezo disc was aligned and pressed on the pump stack. Finally, two syringe needles, 0.65 mm in diameter, were attached to the inlet and outlet by epoxy glue (Araldite, Super rapid epoxy). The assembled pump, measuring 15 mm in diameter and 3.8 mm thick, is shown in Figure 7.

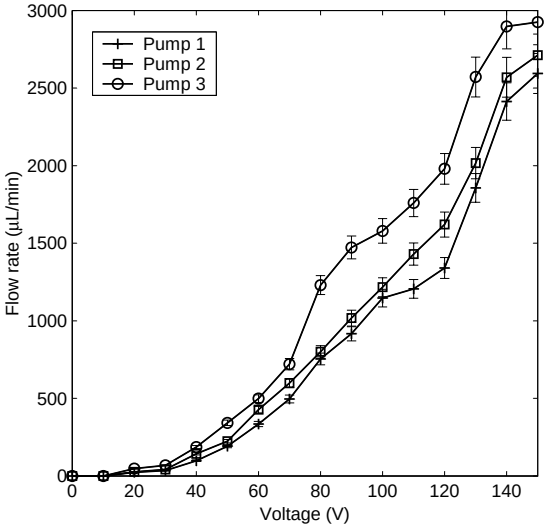

Figure 8: Flow rate versus voltage (frequency=100Hz).

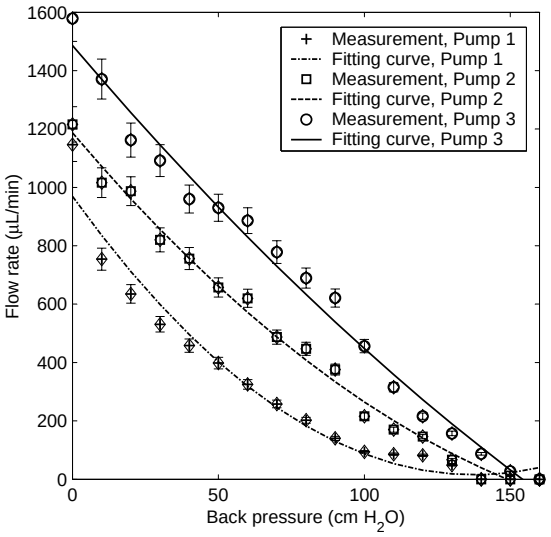

Figure 9: Flow rate versus back pressure (V=100± V, frequency=100Hz).

4 EXPERIMENTAL RESULTS

Three pumps were assembled by the lamination technique described in 3.3. Each micropump was equipped with a micro check valve discussed above. The pumps were characterized using a simple setup described in a previous paper [3]. The working fluid was DI water. The pumps needed to be primed using a syringe before testing. The measurement error is less than 5%. The measured flow rates versus actuating voltages characteristics at the frequency of 100 Hz are shown in Figure 8. Finally, Figure 9 shows the flow rates versus back pressures at ± 100 V and 100 Hz.

The three pumps show significant improvement over the pump reported in [2]. It is evident that the pump's performances are closely related to the spring constants of the valves. Pump 3 has the best performance due to its lowest spring constant. Pump 3 achieved a flow rate up 2.9 ml/min and back pressures up to 160 cm of water (under a voltage of ± 150 V). That is nearly three times the flow rate (1 ml/min) and 8 times the back pressure (0.2 m) of the pump in [2]. Pump 3 delivers almost 24 times of the pumping power compared to the previous pump. The pumping power is estimated by (2).

$$P_{pump} = \frac{Q_{max} \times p_{max}}{2} \tag{2}$$

where P_{pump} is the pumping power, p_{max} and Q_{max} are the maximum back pressure and the maximum flow rate, respectively.

The reasons for the improvements are: better alignment between the two valves and of the valves to the inlet and outlet; better seal between the valve disc and the inlet/outlet thanks to the pre-loaded spring; lower spring constant valve design.

5 CONCLUSION

We have designed, fabricated and characterized the first fully polymeric piezo-actuated micropumps assembled by lamination technique. The main advantages of the pumps are: modular design, low cost, simple fabrication and assembly processes. All fabrication and assembly processes, except for SU-8 parts, were carried out outside clean rooms. Moreover, the pump designs are easily integrated into complex microfluidic systems.

We are further improving the pump design to make it self-priming as well as to use thermal actuation force. Self-priming can be achieved by using thinner PMMA plates, which reducing the pump dead volume. Thermal actuator is being experimented; and shows promising results.

ACKNOWLEDGEMENT

This work was supported by the academic research fund of the Ministry of Education Singapore, contract number RG11/02.

REFERENCES

[1] NT. Nguyen, TQ. Truong, KK. Wong, SS. Ho and LN Low, "Micro check valves for integration into polymeric microfluidic devices," J. Micromech. Microeng., 14, 69–75, 2004.

[2] NT. Nguyen and TQ. Truong, "A fully polymeric micropump with piezoelectric actuator," Sensors and Actuators B, 97, 137–43, 2004.

[3] NT. Nguyen and XY. Huang, "Miniature valveless pumps based on printed circuit board technique," Sensors and Actuators A, 88, 104–11, 2001.